

Quiet swimming at low Reynolds number

Anders Andersen,¹ Navish Wadhwa,¹ and Thomas Kiørboe²

¹*Department of Physics and Centre for Ocean Life, Technical University of Denmark, DK-2800 Kgs. Lyngby, Denmark*

²*National Institute for Aquatic Resources and Centre for Ocean Life, Technical University of Denmark, DK-2920 Charlottenlund, Denmark*

(Received 18 July 2014; published 24 April 2015)

The stresslet provides a simple model of the flow created by a small, freely swimming and neutrally buoyant aquatic organism and shows that the far field fluid disturbance created by such an organism in general decays as one over distance squared. Here we discuss a quieter swimming mode that eliminates the stresslet component of the flow and leads to a faster spatial decay of the fluid disturbance described by a force quadrupole that decays as one over distance cubed. Motivated by recent experimental results on fluid disturbances due to small aquatic organisms, we demonstrate that a three-Stokeslet model of a swimming organism which uses breast stroke type kinematics is an example of such a quiet swimmer. We show that the fluid disturbance in both the near field and the far field is significantly reduced by appropriately arranging the propulsion apparatus, and we find that the far field power laws are valid surprisingly close to the organism. Finally, we discuss point force models as a general framework for hypothesis generation and experimental exploration of fluid mediated predator-prey interactions in the planktonic world.

DOI: [10.1103/PhysRevE.91.042712](https://doi.org/10.1103/PhysRevE.91.042712)

PACS number(s): 47.63.Gd, 47.15.G–

Swimming is essential for feeding and reproduction of many aquatic organisms, as the encounter rates with prey and mates scale with swimming speed [1]. But there is a trade-off since the associated fluid disturbance may risk the survival of the swimmer by signaling its presence to rheotactic predators. Both the magnitude and the spatial decay of the fluid disturbance depend on the distribution of the propulsive forces and the drag forces on the organism [2–5]. The stresslet is the simplest possible model of the far field flow due to a single, freely swimming and neutrally buoyant low Reynolds number swimmer [6,7]. It describes the flow due to two oppositely directed point forces of equal magnitude that act at different points and represent the thrust due to the swimming appendages and the drag on the body of the organism, respectively. The stresslet gives rise to a fluid disturbance that decays as one over distance squared. Experimentally the stresslet has been found to capture the far field flow created by, e.g., the bacterium *Escherichia coli* [8].

For some low Reynolds number swimmers, the fluid forces due to the propulsion apparatus and the drag on the body of the organism cannot appropriately be described by two point forces only [6,7]. In a swimmer model with two point forces, the far field flow will be dominated by a force dipole. However, with three or more point forces, the force dipole term can be made to vanish and the far field flow will then be a force quadrupole that decays as one over distance cubed. Swimming spermatozoa provide such an example if only the middle portion of the flagellum produces thrust, whereas the two ends of the flagellum produce drag [3]. For such arrangements the force quadrupole can be the dominant term. Similarly the squirmer model can give rise to qualitatively different fluid disturbances depending on whether it represents a puller, a pusher, or a neutral swimmer for which the far field flow is a potential dipole [5,9–11]. The differences in the fluid interactions between pullers, pushers, and neutral swimmers have, e.g., been studied for dense suspensions of such squirmers [5].

In the present paper we focus on exploring the fluid disturbances due to low Reynolds number swimmers with

breast stroke type kinematics. Breast stroke swimming is common among small aquatic organisms, and it has evolved independently in diverse taxonomic groups. Many unicellular organisms swim with breast stroke type kinematics [12–14], and the biflagellated green alga *Chlamydomonas reinhardtii* [Fig. 1(a)] has in particular been the subject of measurements and theoretical analysis [15–17]. The jumping ciliate *Mesodinium rubrum* [Fig. 1(b)] is also a breast stroke type swimmer since it propels itself with an equatorial ciliary belt [4]. The crustacean nauplii, e.g., *Acartia tonsa* [Fig. 1(c)], which is one of the most widespread and successful larval forms in nature [18], swim with a breast stroke [19,20], and the adults of the crustacean order Cladocera, e.g., *Podon intermedius* [Fig. 1(d)], are breast stroke swimmers. It has been suggested that the prevalence of breast stroke swimming in nature could be due to its reduced fluid disturbance. For breast stroke swimmers such as *M. rubrum*, *A. tonsa*, and *P. intermedius* the fluid disturbances have been measured using particle image velocimetry to decay as one over distance cubed [20]. This quiet swimming mode is advantageous for organisms that swim to locomote whereas organisms that swim to feed give rise to fluid disturbances with slower spatial decay [20]. Inspired by these observations and further motivated by the relevance of breast stroke swimming to many plankton, we investigate this propulsion method using a point force model in which two appendages, one on each side of the left-right symmetric organism, each generate half of the propulsive force. The model allows us to explore the possibility of modifying the fluid disturbance by repositioning the point forces that represent the propulsion apparatus.

The three-Stokeslet model is our main example (Fig. 2). The point forces 1 and 2, each of magnitude F , represent the forces due to the swimming appendages or flagella and the point force 3, of magnitude $2F$, represents the force due to the body of the organism. All three point forces are acting at points in the xz plane in the negative or in the positive z direction, respectively, and the organism is swimming in the positive z direction. The three-Stokeslet model has been used to successfully

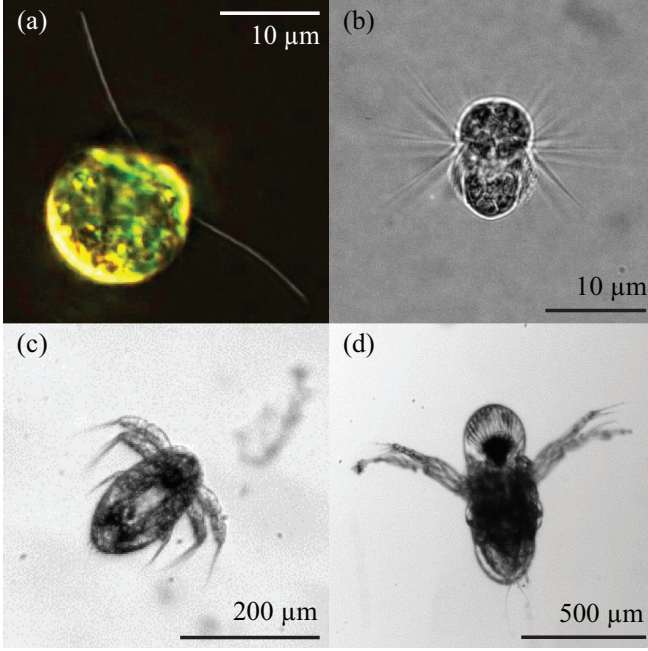


FIG. 1. (Color online) Planktonic breast stroke swimmers across taxonomic groups and sizes: (a) *Chlamydomonas reinhardtii*, a flagellate (image courtesy of Knut Drescher); (b) *Mesodinium rubrum*, a ciliate; (c) a nauplius (juvenile) of *Acartia tonsa*, a copepod; and (d) *Podon intermedius*, a cladoceran. The Reynolds numbers of the swimmers are approximately 10^{-3} , 0.1, 10, and 10, respectively.

model the time-averaged flow field around freely swimming *C. reinhardtii* [15], and we believe that it is an appropriate model for both the near and the far field around other small breast stroke swimmers as well. Due to out of plane appendage motion some breast stroke swimmers rotate around their length axis while swimming. We only consider in-plane and left-right symmetric placement of propulsive forces, because the rotational frequency typically is an order of magnitude

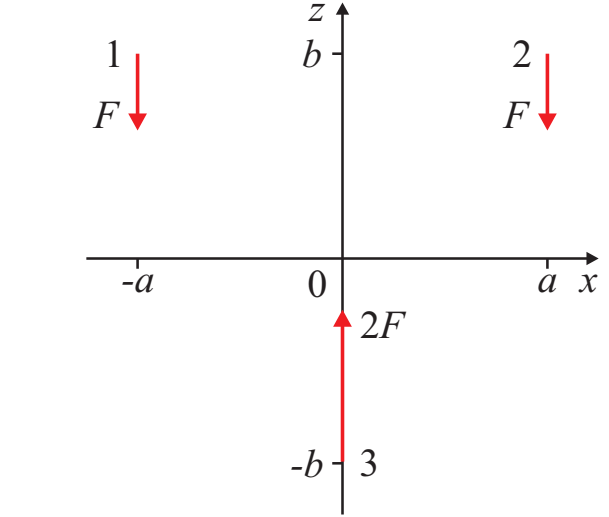


FIG. 2. (Color online) Three-Stokeslet model of a breast stroke swimming aquatic organism. The red vectors represent the point forces.

smaller than the appendage beat frequency and synchronous beating is the dominant mechanism in swimming [19,21].

The basic building block in point force models like the three-Stokeslet model is the low Reynolds number flow due to a point force $\mathbf{F} = (F_x, F_y, F_z)$ which is acting at a source point $\mathbf{x}' = (x', y', z')$. The resulting flow velocity $\mathbf{v} = (v_x, v_y, v_z)$ at the field point $\mathbf{x} = (x, y, z)$ is in index notation

$$v_i(\mathbf{x}) = \frac{1}{8\pi\mu} \left[\frac{F_i}{|\mathbf{x} - \mathbf{x}'|} + \frac{F_j(x_j - x'_j)(x_i - x'_i)}{|\mathbf{x} - \mathbf{x}'|^3} \right], \quad (1)$$

where μ is the dynamic viscosity of the fluid [22]. To describe the flow in the far field where the distance from the origin to the field point $r = (x_i x_i)^{1/2}$ is much larger than the distance from the origin to the source point $r' = (x'_i x'_i)^{1/2}$, we make use of the binomial series and obtain the multipole expansion

$$v_i(\mathbf{x}) = \frac{1}{8\pi\mu} \left[\left(\frac{\delta_{ij}}{r} + \frac{x_i x_j}{r^3} \right) F_j + \left(\frac{x_k \delta_{ij} - x_i \delta_{jk} - x_j \delta_{ik}}{r^3} + \frac{3x_i x_j x_k}{r^5} \right) F_j x'_k + \frac{1}{2} \left(\frac{2\delta_{ik} \delta_{jl} - \delta_{ij} \delta_{kl}}{r^3} - 3 \frac{2\delta_{il} x_j x_k + 2\delta_{jl} x_i x_k + \delta_{kl} x_i x_j - \delta_{ij} x_k x_l}{r^5} + \frac{15x_i x_j x_k x_l}{r^7} \right) F_j x'_k x'_l + \dots \right], \quad (2)$$

where the three terms represent the force monopole, the force dipole, and the force quadrupole, respectively. The strength of the force monopole is described by the force vector F_j , the force dipole by the tensor $p_{jk} = F_j x'_k$, and the force quadrupole by the tensor $t_{jkl} = (1/2)F_j x'_k x'_l$. To determine the total monopole, dipole, and quadrupole terms in the far field flow due to a superposition of N point forces, we add the individual contributions

$$F_j = \sum_{n=1}^N F_{n,j}, \quad p_{jk} = \sum_{n=1}^N p_{n,jk}, \quad t_{jkl} = \sum_{n=1}^N t_{n,jkl}. \quad (3)$$

The strengths depend only on the applied forces and their distribution in space. For a given set of point forces, the dipole

and higher order terms can be modified by rearranging the points of action of the forces. The force multipole solutions are usually used to approximate the far field solution for the flow due to an arbitrarily shaped body with a given surface stress distribution [23], analogous to the approach in electrostatics [24], or as a computational tool [22,25,26].

We now return to the three-Stokeslet model (Fig. 2). We note that the essential parameter in describing the geometry of the point force configuration is the aspect ratio $\alpha = b/a$. The exact velocity field in the model is the sum of the three point force contributions. In the following when plotting the velocity field we use the length scale a and the velocity scale $u = F/(8\pi\mu a)$. Figure 3 shows the velocity fields in the xz plane for $\alpha = 1$, $\alpha = 0.1$, and $\alpha = 0$, respectively. The flows

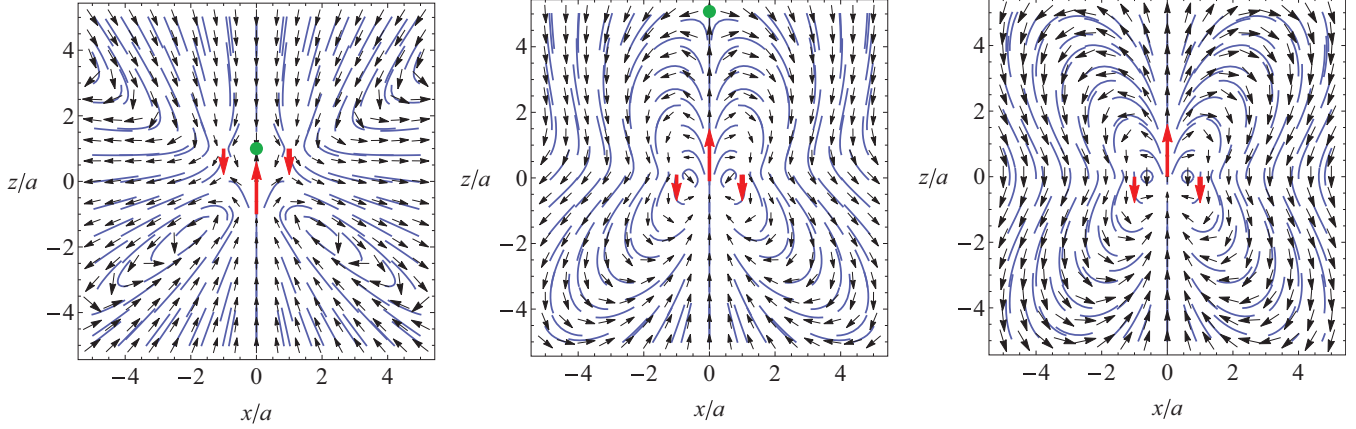


FIG. 3. (Color online) Velocity fields in the three-Stokeslet model: (left) $\alpha = 1$, (middle) $\alpha = 0.1$, and (right) $\alpha = 0$. The thick red arrows represent the point forces and the green dots the stagnation points on the z axis. The flow fields are shown as thin black vectors and blue streamline segments.

in the three cases are qualitatively different. When $\alpha = 1$ two large lateral whirls are present and the flow has a stagnation point on the positive z axis at $z/a = 1$. The stagnation point on the positive z axis is located approximately at $z/a \approx 1/(2\alpha)$ when $0 < \alpha \ll 1$. The stagnation point is therefore at $z/a \approx 5$ when $\alpha = 0.1$. When $\alpha = 0$ the flow on the entire z axis is in the positive z direction and the whirl centers are on the x axis at $x/a = \pm(\sqrt{5} - 1)/2 \approx \pm 0.6180$.

The predicted flow fields for low α values correspond qualitatively with the flow fields measured recently using particle image velocimetry for *A. tonsa* nauplii [27] and *P. intermedius* [20]. Also, the stagnation point on the positive z axis and the two large lateral whirls in the velocity field in the $\alpha = 1$ force configuration are found in the average velocity field observed around the breast stroke swimming *C. reinhardtii* [15]. Similarly, the flows due to our model swimmer with variable α agree qualitatively with the unsteady two-dimensional velocity field measured for *C. reinhardtii* in a thin liquid film [16]. This comparison suggests that unsteady flows around other breast stroke swimmers at low Reynolds number can be captured in quasisteady approximation by the three-Stokeslet model.

The forces in the three-Stokeslet model are pointing in the positive and in the negative z direction, respectively, and because of the left-right symmetry, p_{zz} is the only possible nonzero component of the tensor describing the strength of the force dipole. By adding the three contributions we obtain $p_{zz} = -4Fb$, which depends linearly on b and vanishes when $b = 0$. Similarly we find the only nonzero component of the tensor describing the force quadrupole $t_{zzx} = -Fa^2$. The multipole expansion of the three-Stokeslet velocity field becomes

$$v_x \approx \frac{F}{8\pi\mu} \left[\frac{4bx}{r^3} \left(1 - 3\left(\frac{z}{r}\right)^2 \right) + \frac{3a^2xz}{r^5} \left(3 - 5\left(\frac{x}{r}\right)^2 \right) \right], \quad (4)$$

$$v_y \approx \frac{F}{8\pi\mu} \left[\frac{4by}{r^3} \left(1 - 3\left(\frac{z}{r}\right)^2 \right) + \frac{3a^2yz}{r^5} \left(1 - 5\left(\frac{x}{r}\right)^2 \right) \right], \quad (5)$$

$$v_z \approx \frac{F}{8\pi\mu} \left[\frac{4bz}{r^3} \left(1 - 3\left(\frac{z}{r}\right)^2 \right) + \frac{a^2}{r^3} \left(1 - 3\frac{x^2 - z^2}{r^2} - \frac{15x^2z^2}{r^4} \right) \right]. \quad (6)$$

For the magnitude of the velocity v on the x axis we find asymptotically

$$\frac{v}{u} = \begin{cases} \frac{4\alpha}{|x/a|^2}, & \text{if } \alpha \neq 0, \\ \frac{2}{|x/a|^3}, & \text{if } \alpha = 0, \end{cases} \quad (7)$$

and similarly on the z axis

$$\frac{v}{u} = \begin{cases} \frac{8\alpha}{|z/a|^2}, & \text{if } \alpha \neq 0, \\ \frac{4}{|z/a|^3}, & \text{if } \alpha = 0. \end{cases} \quad (8)$$

We find that the expressions provide good approximations of the flow for $r/a > 3$ when $\alpha = 1$ and $\alpha = 0$ (Fig. 4). The force dipole dominates for $r/a \gg 1/\alpha$ when $\alpha \neq 0$, and the magnitude of the flow velocity therefore decays as one over distance squared for $r/a > 3$ when $\alpha = 1$. In contrast the force dipole is eliminated when $\alpha = 0$ and the magnitude of the flow velocity is well described by the force quadrupole and decays as one over distance cubed. Asymptotically we find on both the x axis and the z axis that $v_{\alpha=1}/v_{\alpha=0} = 2(r/a)$, and as an example we therefore have $v_{\alpha=1}/v_{\alpha=0} \approx 10$ when $r/a = 5$. This shows that the fluid disturbance is reduced significantly by positioning the propulsion apparatus appropriately. When $\alpha = 0.1$ the far field flow for $r/a > 10$ is dominated by the force dipole, but comparison with the far field expressions (7) and (8) shows that the magnitude of the flow velocity in the intermediate range $3 < r/a < 10$ is dominated by the force quadrupole and the fluid disturbance is small and comparable to the situation when $\alpha = 0$.

Our study has demonstrated that by appropriately arranging its propulsion apparatus a breast stroke swimmer produces only a small fluid disturbance with a fast spatial decay as observed experimentally for breast stroke swimming plankton such as *M. rubrum*, *A. tonsa* nauplii, and *P. intermedius* [20]. Breast stroke swimming may thus be advantageous in the

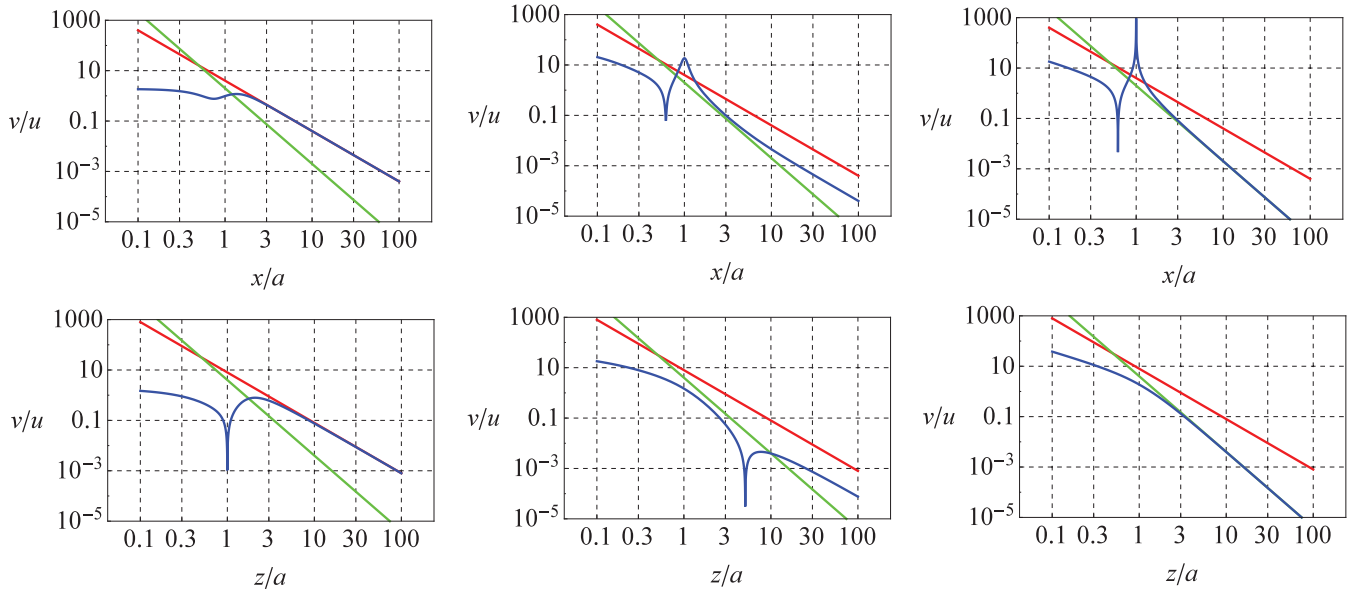


FIG. 4. (Color online) Magnitude of the velocity in the three-Stokeslet model (blue) on the positive x axis (top) and the positive z axis (bottom) with $\alpha = 1$ (left), $\alpha = 0.1$ (middle), and $\alpha = 0$ (right). Also shown are the far field approximations (7) and (8) for $\alpha = 1$ (red, r^{-2} decay) and $\alpha = 0$ (green, r^{-3} decay).

small-scale blind world of the plankton, where predator and prey perception is often mediated by fluid signals. We note, however, that our low Reynolds number model does not apply strictly to *A. tonsa* nauplii and *P. intermedius* since the Reynolds numbers of the swimmers are approximately 10 (Fig. 1). In the three-Stokeslet model with $\alpha \neq 0$, the force dipole term always dominates the far field region $r/a \gg 1/\alpha$, but the transition range, in which the force quadrupole term is dominant, extends farther and farther out as α is decreased to zero. In breast stroke swimming the propulsive forces are delivered during the entire beat of the swimming appendages, corresponding to different points of action of the forces. However, we presume that the highest propulsive forces are created in the middle of the power stroke when α is small and that our conclusions for breast stroke swimming are therefore robust.

Any small density mismatch of the organism will lead to a Stokeslet term that will dominate far away from the organism farther than some distance Λ . For an organism with a stresslet term one finds $\Lambda/a \sim F/F_g$, where F_g is the buoyancy corrected gravitational force on the swimmer [15], and for a quiet swimmer we estimate $\Lambda/a \sim (F/F_g)^{1/2}$. With a given density mismatch the Stokeslet term will be most significant for large organisms since the buoyancy corrected gravitational force is proportional to the volume of the organism, whereas the propulsive forces are roughly proportional to the length of the organism squared [28]. For a low Reynolds number swimmer to be quiet we must therefore have that both the density mismatch and the size of the organism are so small that the Stokeslet term only dominates far from the organism where the fluid disturbances are so small that they are irrelevant for any interaction with other organisms.

Reducing the flow disturbance generated by a swimming organism not only hides it from rheotactic predators, it also improves the chances of the organism capturing small prey. An organism moving towards a prey has to ensure that the

prey is not warned and pushed away by the flow created by the organism. Millimeter sized planktonic organisms like copepods can do this by reducing the extent of the viscous boundary layer around them by moving quickly and achieving a Reynolds number sufficiently above unity [29]. Our analysis shows that it is also possible for low Reynolds number swimmers to reduce their induced flow disturbance, thereby allowing them to approach small prey quietly.

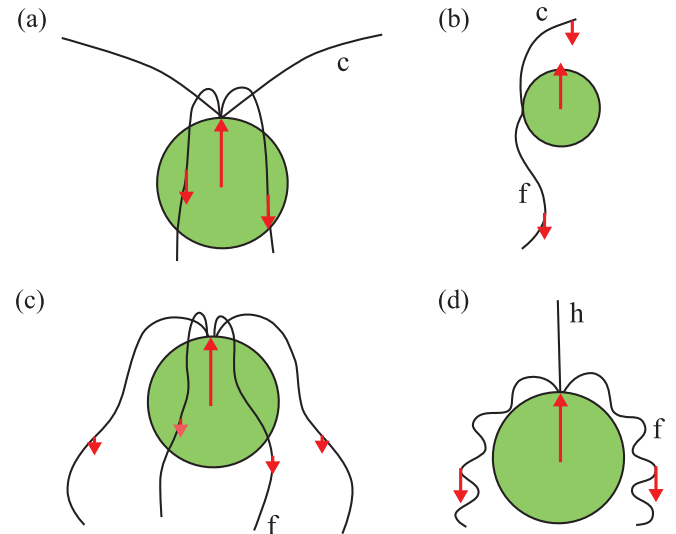


FIG. 5. (Color online) Micro-organisms with multiple flagella. In all cases the swimming direction is upwards, and the red vectors represent approximately the forces. The flagella function with either a flagellar beat, f , or a ciliary beat, c . Protists with (a) two pairs of flagella that beat out of phase, e.g., *Carteria*, (b) a leading and a trailing flagellum, e.g., *Nephroselmis*, and (c) all four flagella pushing steadily, e.g., *Cymbomonas* [13]. (d) A haptophyte with two flagella and a haptonema, h , in the front, e.g., *Chrysochromulina* [12].

Point force models should be used with care since they do not always capture the flow close to the swimmer [8], but for some swimmers they provide a powerful tool that can also capture the near field fluid disturbance surprisingly well [15]. In addition to the breast stroke swimmers there are many examples of aquatic organisms with multiple flagella for which the point force framework could form the basis for theoretical analysis. Figure 5 shows sketches of selected unicellular organisms reproduced after Refs. [12,13]. Organisms with flagella acting on the sides [Figs. 5(a) and 5(c)] may eliminate the force dipole term by locating the propulsive forces in the same transversal plane as the net drag force, and organisms with a leading and a trailing flagellum [Fig. 5(b)] may eliminate the force dipole term by suitably adjusting the two propulsive forces. We therefore speculate that all three arrangements of the propulsion apparatus might allow the organisms to swim quietly. Also the haptoneema in the haptophyte [Fig. 5(d)],

which is used to capture prey, might be so located that its tip reaches the region beyond the forward stagnation point, thus aiding it in encountering the prey entrained in the downwards flow. It would be interesting in future studies to experimentally explore the flows around such organisms.

Predator-prey interactions govern the structure and function of (pelagic) food webs. The idealized model framework can therefore be used for hypothesis generation and experimental exploration of concrete predator-prey interactions mediated by fluid signals among planktonic organisms with different arrangements of the propulsion apparatus and, thus, to more fully understand the functioning of pelagic food webs.

We thank Lasse Tor Nielsen for drawing our attention to Refs. [12,13]. The Centre for Ocean Life is a VKR center of excellence supported by the Villum Foundation.

-
- [1] T. Kiørboe, *A Mechanistic Approach to Plankton Ecology* (Princeton University Press, Princeton, 2008).
- [2] H. Jiang and G.-A. Paffenhöfer, *Mar. Ecol.: Prog. Ser.* **373**, 37 (2008).
- [3] D. J. Smith and J. R. Blake, *Math. Sci.* **34**, 74 (2009).
- [4] H. Jiang, *J. Plankton Res.* **33**, 998 (2011).
- [5] J. J. Molina, Y. Nakayama, and R. Yamamoto, *Soft Matter* **9**, 4923 (2013).
- [6] E. Lauga and T. R. Powers, *Rep. Prog. Phys.* **72**, 096601 (2009).
- [7] J. S. Guasto, R. Rusconi, and R. Stocker, *Annu. Rev. Fluid Mech.* **44**, 373 (2012).
- [8] K. Drescher, J. Dunkel, L. H. Cisneros, S. Ganguly, and R. E. Goldstein, *Proc. Natl. Acad. Sci. USA* **108**, 10940 (2011).
- [9] M. Lighthill, *Commun. Pure Appl. Math.* **5**, 109 (1952).
- [10] J. R. Blake, *J. Fluid Mech.* **46**, 199 (1971).
- [11] T. Ishikawa, M. P. Simmonds, and T. J. Pedley, *J. Fluid Mech.* **568**, 119 (2006).
- [12] M. A. Sleigh, *BioSystems* **14**, 423 (1981).
- [13] I. Inouye and T. Hori, *Protoplasma* **164**, 54 (1991).
- [14] D. Bray, *Cell Movements: From Molecules to Motility*, 2nd ed. (Garland Science, New York, 2001).
- [15] K. Drescher, R. E. Goldstein, N. Michel, M. Polin, and I. Tuval, *Phys. Rev. Lett.* **105**, 168101 (2010).
- [16] J. S. Guasto, K. A. Johnson, and J. P. Gollub, *Phys. Rev. Lett.* **105**, 168102 (2010).
- [17] D. Tam and A. E. Hosoi, *Proc. Natl. Acad. Sci. USA* **108**, 1001 (2011).
- [18] J. W. Martin, J. Olesen, and J. T. Høeg, *Atlas of Crustacean Larvae*, edited by J. W. Martin, J. Olesen, and J. T. Høeg (Johns Hopkins University Press, Baltimore, MD, 2014), pp. 8–16.
- [19] C. M. Andersen Borg, E. Bruno, and T. Kiørboe, *PLoS One* **7**, e47486 (2012).
- [20] T. Kiørboe, H. Jiang, R. J. Gonçalves, L. T. Nielsen, and N. Wadhwa, *Proc. Natl. Acad. Sci. USA* **111**, 11738 (2014).
- [21] M. Polin, I. Tuval, K. Drescher, J. P. Gollub, and R. E. Goldstein, *Science* **325**, 487 (2009).
- [22] C. Pozrikidis, *Boundary Integral and Singularity Methods for Linearized Viscous Flow* (Cambridge University Press, Cambridge, UK, 1992).
- [23] S. Kim and S. J. Karrila, *Microhydrodynamics: Principles and Selected Applications* (Butterworth-Heinemann, Boston, 1991).
- [24] J. D. Jackson, *Classical Electrodynamics*, 3rd ed. (Wiley, New York, 1999).
- [25] C. Pozrikidis, *Introduction to Theoretical and Computational Fluid Dynamics*, 2nd ed. (Oxford University Press, Oxford, U.K., 2011).
- [26] L. G. Leal, *Advanced Transport Phenomena* (Cambridge University Press, Cambridge, UK, 2007).
- [27] N. Wadhwa, A. Andersen, and T. Kiørboe, *J. Exp. Biol.* **217**, 3085 (2014).
- [28] T. Kiørboe, *Biol. Rev.* **86**, 311 (2011).
- [29] T. Kiørboe, A. Andersen, V. J. Langlois, H. H. Jakobsen, and T. Bohr, *Proc. Natl. Acad. Sci. USA* **106**, 12394 (2009).